Solar Energy 259 (2023) 235–245

Contents lists available at ScienceDirect

Solar Energy

journal homepage: www.elsevier.com/locate/solener

A novel method for the site selection of large-scale PV farms by using AHP and GIS: A case study in İzmir, Türkiye

Abdullah Demir [a], Ali Ersin Dinçer [b,*], Kutay Yılmaz [c]

[a] Dep. of Civil Eng., Structural Laboratory, Abdullah Gül University, Kayseri 38080, Turkey
[b] Dep. of Civil Eng., Hydraulics Laboratory, Abdullah Gül University, Kayseri 38080, Turkey
[c] Alter International Engineering and Consultancy Inc., Ankara, Turkey

ARTICLE INFO

Keywords:
Photovoltaic plants
Large-scale PV site selection
AHP
GIS
Site selection
Solar PV

ABSTRACT

Effective and sustainable climate-friendly policies to reduce carbon dioxide emissions in line with the 2020 European Green Deal are necessary. Accordingly, renewable energies assumed a critical role, rendering the site selection of these systems very crucial. The present study proposes a novel approach to the site selection of large-scale photovoltaic (PV) plants using a combination of analytic hierarchy process (AHP) and geographic information system (GIS). In the study, the weights of criteria used for selecting solar PV panels are adjusted according to the installed capacity of the PV plant. The land of cost is included as a criterion in the AHP for the first time in PV plant site selection. Besides, a novel method called optimality-based site growing (OBSG) is introduced to further analyze the suitable sites obtained from GIS simulations and to determine the most suitable locations of PV farms. The proposed method is demonstrated with a case study of Türkiye, and the results show that the method effectively determines the most suitable locations for large-scale PV plants.

1. Introduction

Climate-friendly policies are necessary to reduce the emissions targeted in 2020 European Green Deal [17]. The most effective and sustainable policies are the investments on renewable energies [12] as fossil fuels cover over 40% of energy-related carbon dioxide emissions [47]. Among the renewable energy sources solar energy could be the best option due to being the most abundant and not exhaustible energy source [22]. In addition, unlike wind energy, acceptance of solar energy by the population is very high and more preferrable than other renewable energy sources [13,42]. The higher acceptance of solar energy can be attributed to concerns regarding noise pollution, visual impact, and potential harm to wildlife caused by wind turbines, as well as the advantages of solar energy, including widespread availability, versatile installation options, aesthetic appeal, and advancements in technology that have improved affordability and accessibility [6]. Furthermore, the impact of utilization of solar energy on ecosystem is trivial [22]. For these reasons, many countries have been planning their solar energy strategies [18]. Policy makers take into account a variety of crucial factors when making decisions regarding the investment of solar photovoltaic (PV) plants [3]. These factors can be categorized into several key areas, including political, social, economic, technical, and environmental considerations [7]. The selection of the location of solar PV plants should encompass all these factors [33].

Different methods have been incorporated with geographic information system (GIS) for the optimum site selection of solar PV plants. These methods are fuzzy logic models [15,28,48], multi-criteria decision-making (MCDM) methods such as the Analytical Hierarchy Process (AHP) [1,10,14,19,5,34], Step-wise Assessment Ratio Analysis (SWARA) [9], the Decision-Making Trial and Evaluation Laboratory (DEMATEL) [37] or the Elimination and Choice Translating Reality [36] and hybrid methods [8,15]. Across all methodologies, specific criteria that influence the identification of favorable locales for solar PV plant installation, as well as restricted zones where construction is not permitted, are established. Subsequently, geospatial analyses are conducted via GIS to ascertain and prioritize suitable sites. In all the methods the criteria affecting the suitable locations as well as the restricted zones that PV plants cannot be constructed are determined. Then GIS works are performed to determine and rank the suitable sites. In the present study, the AHP method is preferred due to its advantages such as the quantification of qualitative attributes or reducing cognitive errors [39]. Since many criteria are qualitative in the selection of suitable sites for PV plants, quantification of the criteria is necessary. The AHP has also advantages over other MCDM methods. While the

* Corresponding author.
E-mail addresses: abdullah.demir@agu.edu.tr (A. Demir), ersin.dincer@agu.edu.tr (A.E. Dinçer).

https://doi.org/10.1016/j.solener.2023.05.031
Received 17 April 2023; Received in revised form 9 May 2023; Accepted 19 May 2023
Available online 23 May 2023

SWARA's capacity to identify the degree of consistency is limited, the DEMATEL method requires large number of pairwise comparisons [19,31]. Criteria used in the AHP method are determined considering the studies in the literature, expert opinions, and special characteristics of the study area.

Although the number of studies for the site selection of PV plants is high [10,43,44,46], there are limited number of studies focusing on the site selection for large-scale solar PV farms, typically characterized by solar power plants that produce a minimum of 5 MW of energy [3,4,23]. In [26], the suitable sites for large ground-mounted PV plants were located with the help of a GIS tool and an artificial neural network (ANN) for Piedmont region of Italy. Instead of using the data in the literature or conducting a survey analysis, technical documents were used while defining the criteria affecting the site selection process. [24,25] investigated suitable areas for the large-scale PV plants using the AHP method incorporating with GIS in a case study for Eastern Morocco. The method they used is appropriate for PV plants independent from the installed capacity and no manipulation was proposed to deal with large-scale PV plants. Similarly, [33] used MCDM and GIS tools to select the best locations for implementation of large-scale PV plants in Brazil. The effect of the size of PV plants is included in the criteria selection process using the systematic review of the literature proposed in [32]. A ranking from the best to the worst area for the large-scale PV plants was generated and the areas were classified according to this ranking. The results they found were the areas instead of pixels mainly due to the tool calculating the relative proximity to the ideal solution among various alternatives, so that the locations where large-scale PV plants can be constructed were clearly shown. In [41], possible sites for large-scale wind and solar farms were selected for Israel using AHP-GIS method. Solar appropriate sites less than 5 km^2 were excluded from the analysis results so that larger sites to locate large-scale PV plants were obtained. As can be seen, in previous studies there were attempts to find large areas to construct large-scale PV plants. In the present study, a novel method is proposed to find the most suitable locations for large-scale PV plants.

In this study, the AHP method is used to prioritize the criteria and GIS is preferred to select the suitable sites of large-scale PV plants. The main novelties of the present study can be pointed out as: Firstly, the weights of criteria used for selecting large-scale solar PV panels are adjusted based on the installed capacity of the PV plant. The relative importance of certain criteria varies depending on the installed capacity. For instance, distance to roads or transmission lines holds more significance for PV plants with lower capacity due to their higher relative costs compared to the total cost. On the contrary, as the capacity increases, the weight assigned to the land cost constraint increases due to the higher construction cost of the PV farm. Secondly, the land cost is included in the criteria list of the site selection of large-scale PV plants for the first time. The land cost is especially important when the installed capacity is higher while it may not be considered when the installed capacity is low. Finally, a novel method called as optimality-based site growing (OBSG) is proposed. In OBSG method, the suitable sites obtained from GIS simulations are further analyzed and the pixels showing the suitable areas are combined with the help of an optimality condition. Therefore, the most suitable locations of large-scale PV farm can be found. In addition, the method ranks the suitable locations by determining sequential optimum locations.

2. Methodology

2.1. Site properties

Izmir is a city located in western Türkiye, on the Aegean coast at the geographical coordinates of 37° 75′ and 39° 50′ N and 26° 00′ and 28° 50′ E. It is the third-most populous city in Türkiye, with a population of over 4 million people. The city is situated on a large bay and is surrounded by mountains, making it a popular tourist destination. The city has a Mediterranean climate, with mild winters and hot summers. The temperature in İzmir Province varied between 2.2 and 28 °C on a monthly basis, on average [2]. The location of İzmir is shown in Fig. 1.

There are several solar power plants that have been built or are being planned in İzmir, Türkiye. These solar power plants range in size from small-scale rooftop installations to large-scale solar PV farms.

The reasons why İzmir may be a good location to build large capacity solar PV farms can be summarized as follows:

- High solar radiation potential: İzmir has a high solar radiation potential, which is necessary for the efficient operation of solar PV farms[40]. The average solar radiation in the city is among the highest in Türkiye. This high solar radiation potential makes Izmir an attractive location for solar power generation.
- Government support: The Turkish government set ambitious targets for the country's renewable energy sector, so renewable energy production has increased significantly in recent years, with a three-fold increase in the past decade. Türkiye has already surpassed its goal of 38.8% of power generation from renewable sources outlined in its Eleventh Development Plan for the years 2019–2023. The country plans to continue promoting renewable energy and will add 10 GW of solar and wind capacity between 2017 and 2027 [20].
- Growing renewable energy market: Türkiye's renewable energy market is growing rapidly [27], and there is a strong demand for solar power. This presents an opportunity for companies to invest in the development of large capacity solar PV farms in the country.
- Proximity to major cities and industries: Izmir is a major economic center in Türkiye [21], and it is home to several industries, including textiles, food processing, and chemicals. The city's proximity to these industries and its large population provides a ready market for the electricity generated by solar PV farms.
- Infrastructure: Izmir has a major port and an international airport, which makes it easy to transport solar PV equipment and components to the site, as well as to export the electricity generated by the solar farm. Additionally, the city has a good road network, and it is well connected to the rest of the country [21], which facilitates the integration of the solar power generated into the national grid.

2.2. The AHP method

The AHP method was proposed by Saaty[35]for organizing and analyzing complex decision-making problems. In the AHP, firstly the goal (determination of the suitable sites for PV plants) is defined. Then, the hierarchical structure of the criteria and the pairwise comparison matrix are established, and the comparisons are utilized by using a scale showing the dominance of one criterion over another [34]. After that, the elements of each column are divided by the sum of that column and the sum of the obtained values is divided by the total number of elements in the row. Finally, consistency ratio, *CR*, is calculated according to the following formula.

$$CR = \frac{CI}{RI} \tag{1}$$

$$CI = \frac{\lambda_{max} - n}{n - 1} \tag{2}$$

where *CI* is the consistency index, λ_{max} is the principal eigenvalue and n is the number of criteria used in the AHP process. If the value of consistency ratio is less than 0.10, the inconsistency of the AHP is acceptable.

2.3. Optimality-based site growing (OBSG)

A large-scale PV farm covers a large terrain which could consist of different suitability evaluations. In this regard, this study proposes a novel approach, termed OBSG, that diverges from conventional

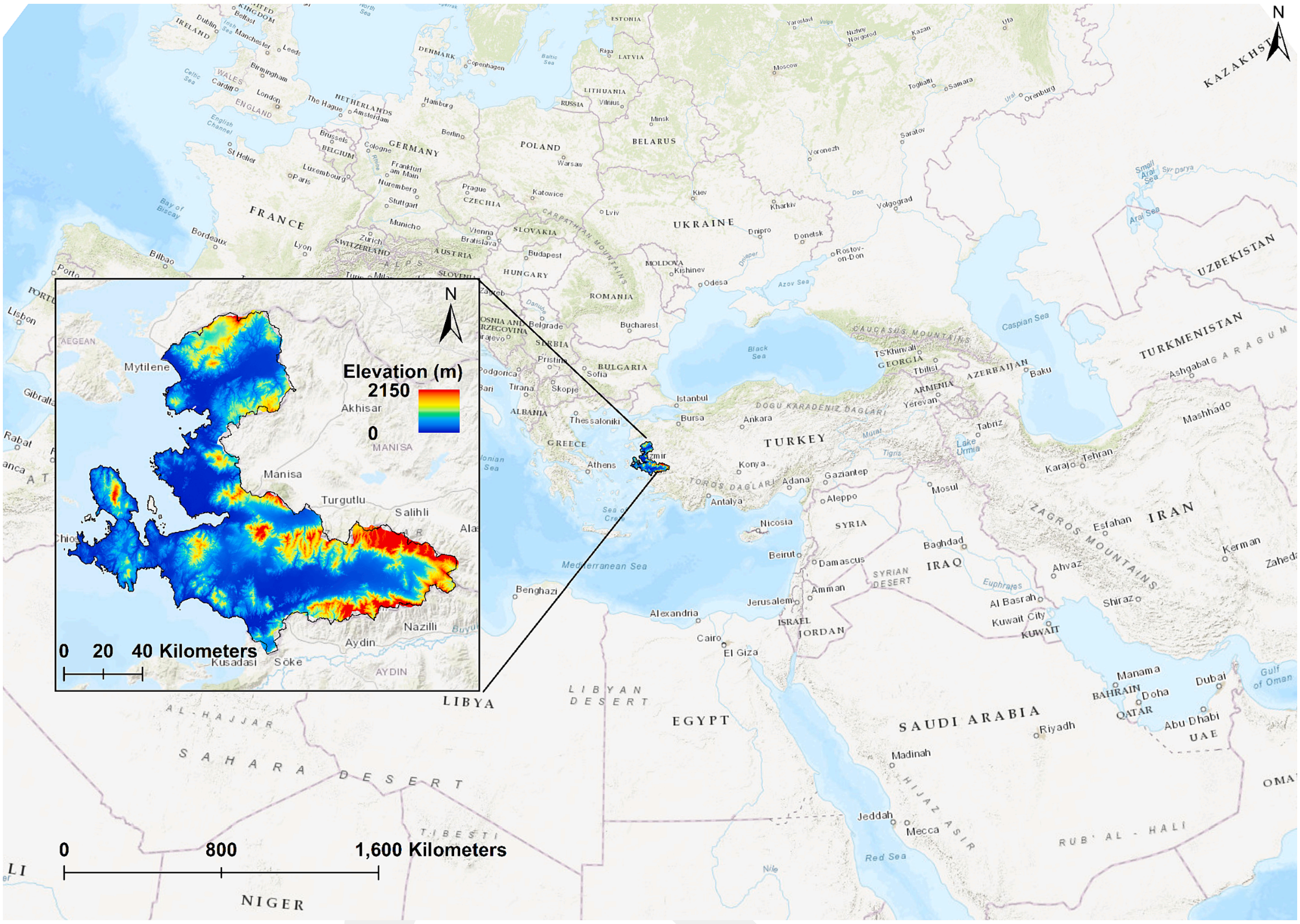

Fig. 1. Digital Elevation Map of İzmir [16] and World Topographic Map (ESRI, USGS).

practices of simply delineating feasible locations for a large-scale PV farm. Rather, the OBSG method defines an optimal site based on a holistic consideration of the terrain covered by the farm.

In OBSG procedure, there are two optimality conditions. The first one is the suitability evaluation result and the second one is the distance from the geometric center which is calculated for the recent circumstance. Starting from a seed point on the map, the site is grown considering these optimality conditions. The optimal site to enlarge is selected among all possible sites adjacent to the current area. The ranking of adjacent sites is based on the assumption of a linear correlation between the optimality criteria.

In the application, the suitability map is colored differently for restricted areas ($C(x,y) = 20$), 0–20% suitability ($Suit = 0.1$ for $C(x,y) = 121$), 20–40% suitability ($Suit = 0.3$ for $C(x,y) = 191$), 40–60% suitability ($Suit = 0.5$ for $C(x,y) = 134$), 60–80% suitability ($Suit = 0.7$ for $C(x,y) = 81$, $Suit = 0.1$) and 80–100% suitability ($Suit = 0.9$ for $C(x,y) = 35$). A random seed point is selected on the suitability map among the most suitable sites of which $C(x,y) = 35$. Then, the score of each adjacent site is calculated dividing the suitability of the site, *Suit*, by the distance, *Dist*, of the site from the geometric center, P_{GC}. The optimal site for expansion is selected based on the highest score among all possible adjacent sites. The enlarging process is carried out till the necessary area, *arneed* is selected. The optimality score (*OS*) of a randomly selected seed point can be calculated through the given flowchart in Fig. 1.

In order to identify the best location for a PV farm, a sequence of optimality scores is obtained by selecting new seed points and recalculating scores. The most suitable site for the PV farm is determined by selecting the site with the highest optimality score from among the feasible options. To obtain a comprehensive view of the optimality scores across the entire map, the flow chart depicted in Fig. 2 is applied to every suitable site on the suitability map. Moreover, a sequential optimal location can be determined by revising the suitability map in each cycle of achievement. The OBSG method is coded using Matlab and integrated with ArcGIS software to carry out GIS operations.

The present study focuses on solar PV panels with capacities of 250 MW, 500 MW, and 1000 MW. Analyzing the Karapınar solar PV plant in Konya, Türkiye, it is observed that an approximate land area of 20 km^2 is required for an approximate capacity of 1350 MW. Consequently, solar PV plants with capacities of 250 MW, 500 MW, and 1000 MW would need land areas of 3.75 km^2, 7.5 km^2, and 15 km^2, respectively.

2.4. Constraints and classification

Every site has its own properties. Thus, constraints should be specified accordingly. The decision criteria are typically determined by considering the objectives of the study, the availability of the georeferenced database, and existing literature [3]. Based on the commonly utilized criteria found in the literature, six constraints have been chosen for the construction of a large-scale PV farm in İzmir. These constraints are solar radiation rate, land use, slope, distance to transmission line, land cost and distance to road.

The study classifies defined constraints into two groups based on their interrelations. Specifically, cost-based interrelations exist among the distance to transmission line, land cost, and distance to road, whereas site-based constraints lack such interrelations in terms of

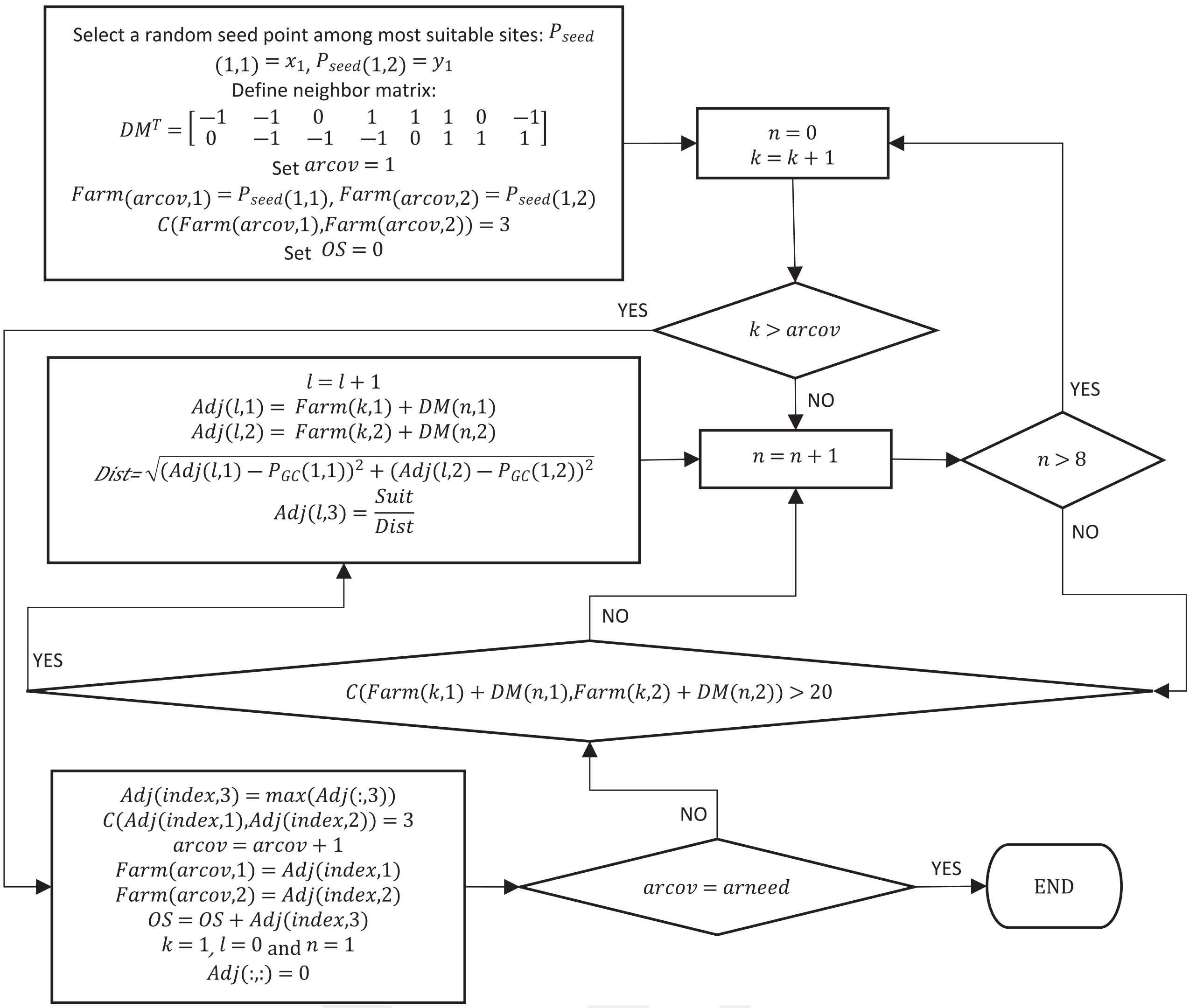

Fig. 2. Flowchart for calculating the position and the optimality score of the PV farm.

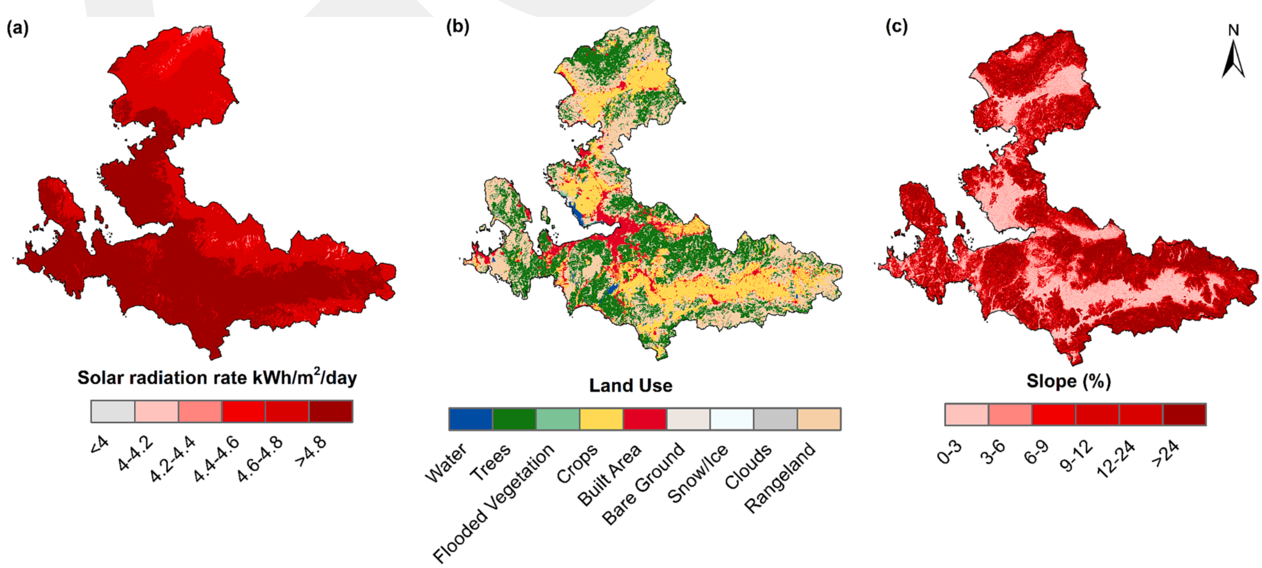

Fig. 3. Maps of solar radiation rate [45], land use [11] and slope.

monetary cost. The weights assigned to each group of constraints are determined through expert judgement. Specifically, the weights for the site-based and cost-based groups of constraints are both set at 0.5, indicating equal importance.

2.4.1. Solar radiation rate

Solar radiation is a crucial factor in determining the potential of a site for solar power generation [24,25]. The amount of solar radiation that a site receives directly affects the output of a solar power plant. In general, sites with higher levels of solar radiation generates more electricity than sites with lower levels of solar radiation. Therefore, when selecting a site for a solar power plant, it is important to consider factors that may affect the amount of solar radiation the site receives such as latitude, altitude, and the presence of nearby shading sources. As shown in Fig. 3a, the solar radiation rate of İzmir is high making the city favorable for PV installation.

2.4.2. Land use

Land use is a crucial factor in the site selection of solar PV farms, as it can greatly impact the overall efficiency and cost-effectiveness of the solar farm. Site selection should take into account the land use that is already happening on the land. For example, if the land is being used for agriculture, it may be more difficult to install solar panels without disrupting the existing use of the land. Also, if the land is already developed, it may be more expensive to acquire and prepare the land for solar PV installation. To define the best regions, the land use utilized from Sentinel-2 Satellite imagery was used and shown in Fig. 3b.

2.4.3. Slope

A flat site with little to no slope is ideal for solar PV installation as it allows for easy installation and maintenance of the panels [7]. However, if a flat site is not available, a site with a slight slope can also be used. On the other hand, a site with a steep slope can be more challenging to work with and may not be the best choice for a solar PV farm. This is because, a steep slope can cause issues with drainage and erosion and can also make it difficult to install and maintain the solar panels. Additionally, areas with steep slopes are not favorable due to their limited economic viability [4]. The topography of İzmir, characterized by mountains aligned perpendicular to the sea, resulted in the creation of the slope map shown in Fig. 3c. In the present study, restrictions were imposed on the installation of PV panels in areas where the slope exceeds 24% [44].

2.4.4. Land cost

The cost of land can be a significant factor in the site selection of solar PV farms as it can significantly impact the overall costs and profitability of a project. A lower land cost can make a site more attractive to developers, as it will lower the costs of the project and increase the potential return on investment. Additionally, land cost can also affect the feasibility of a project, as a high cost may push the project's costs above the threshold for it to be financially viable. For these reasons, the land cost, both with and without eligibility for urban development, was calculated by considering approximate costs determined by the relevant county or district municipalities. It is important to note that the cost of lands was obtained in text format and the average cost of land was spatially distributed across the district polygons in the GIS environment. Once the distribution process was completed, the polygons were converted to raster format for further analysis. The resultant land cost values are shown in Fig. 4a.

2.4.5. Distance to transmission line

Closer proximity to transmission lines can make it easier and less costly to connect the solar farm to the grid, as the distance and cost of running power lines from the solar farm to the transmission lines will be less [38]. To address this concern, the current study incorporates the distance to energy transmission lines as a factor in the site selection process as shown in Fig. 4b.

2.4.6. Distance to road

The farther the site is from a road, the more expensive it will be to transport equipment and materials to the site. Additionally, access to the site for maintenance and repair can also be more difficult and costly if it is located far from a road. In order to mitigate risks associated with road accidents such as collisions and fires, it is common practice for most studies to exclude areas located very close to roads. In the present study, the restricted distance to the road is taken as 25 m. The vector data for road networks, which includes highways, primary and secondary roads, as well as rural roads and their links, were obtained from OpenStreetMap (OSM). Distance to road was classified and its geographic distribution is given in Fig. 4c.

2.5. Restricted areas

Restrictions should be specified correctly according to the conditions of the site. Some restrictions are obligated by the government. In contrast, some restrictions are specified by the experts based on the environmental, economic and safety issues. It is not possible to build anything on the national parks, military zones, cemeteries, forests etc. In contrast, although it is not restricted by the government, water and crops were restricted due to environmental effects. In addition, built area, snow/ice, steep slopes and sites nearby the roads were also

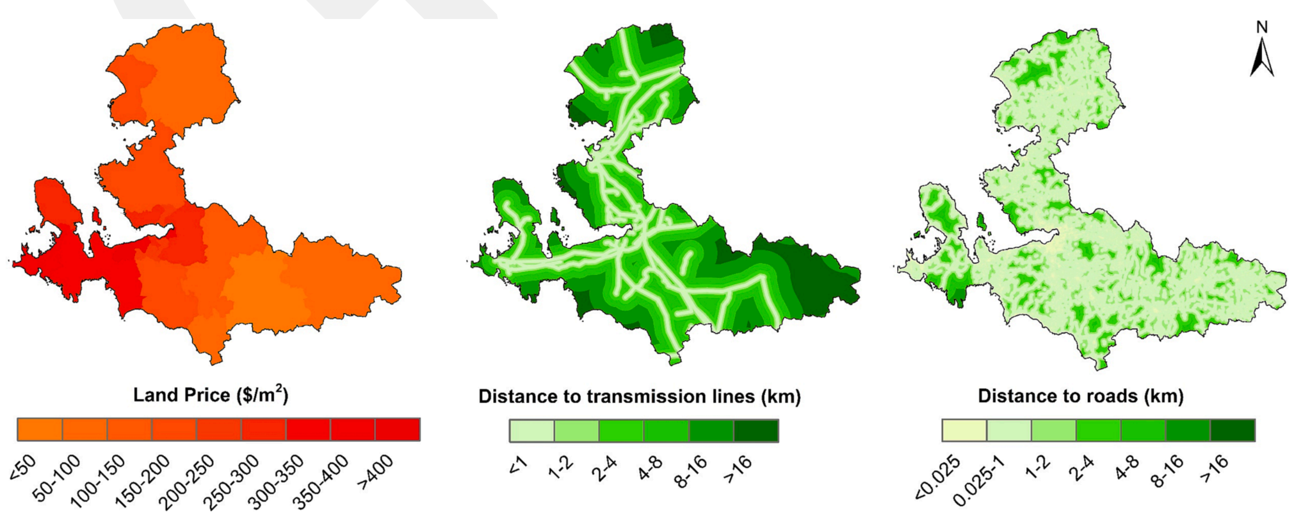

Fig. 4. Maps of land price, distance to transmission lines and distance to roads [30].

restricted.

2.6. Determination of weights of constraints

The constraints can be divided into two distinct categories: site-based and cost-based. This categorization facilitates the establishment of more objective connections between the various constraints. Initial AHP constants of site-based and cost-based constraints are given in Table 1 and Table 2, respectively. The weights for each group (refer to Table 3 and Table 4) was determined using the conventional AHP method. The total weight for each group was found to be 0.5, as determined through an expert survey. The pair-wise comparison matrices shown in Table 1 and Table 2 were established for determining the criteria weights, taking into account the reasoning and significant weights assigned to criteria in similar studies on solar site suitability [10,29,44].

The weights of constraints in the site-based group remain constant across different capacity levels, while those in the cost-based group are impacted by changes in capacity. Specifically, the cost of constructing a PV farm increases with capacity, resulting in a corresponding increase in the weight assigned to the land cost constraint. In contrast, the cost of constructing a power line and road for a given site remains unchanged, resulting in a decrease in the weight assigned to these constraints as capacity increases. These findings are summarized in Table 2, which details the constants matrix for each level of capacity up to a maximum of 1000 MW. The impact of capacity on the weights of constraints is further demonstrated in Table 4, which displays the resulting weights for each constraint at different levels of capacity. As expected, the weight assigned to the land cost constraint increases as capacity increases, while the weights of other cost-based constraints decrease. It is worth noting that although the cost of constructing a power line and road to a given site remains constant, the weights of these constraints also decrease due to the condition that the summation of weights in the cost-based group should be 0.5.

As previously stated, the weights assigned to each group in the decision-making process were determined based on the similar studies available in the literature and expert judgement and set at 0.5. In order to investigate the potential impact of the capacity of the PV farm on these weights, a survey was conducted among a panel of 50 experts. Specifically, respondents were asked to indicate whether they believed that the weights assigned to each group would be affected by the capacity of the PV farm. The results of the survey revealed that 40% of the experts believed that the weights of the groups would be impacted by the capacity of the PV farm, while the remaining 60% did not hold this view. While the proportion of experts indicating that there may be an impact was not deemed entirely satisfactory, the overall findings were sufficient to suggest that the relationship between the groups would not be undermined by an increase in the capacity of the PV farm.

Weights of each set of constraints are tabulated in Table 5. In addition, the sub-criteria of each constraint and indicators are given in the same table.

3. Results

The AHP method was used to derive weights for each constraint in two distinct groups – site-based and cost-based. The resulting weights, presented in Table 5, were then utilized in a series of spatial analyses conducted using ArcGIS software to develop suitability maps for different capacities of large-scale PV farms. Specifically, analyses were conducted for capacities of 250 MW, 500 MW, and 1000 MW.

Table 1
AHP constants of site-based constraints.

	Solar radiation rate	Land use	Slope
Solar radiation rate	1	2	4
Land use	0.5	1	3
Slope	0.25	0.333	1

Table 2
AHP constants of cost-based constraints for different capacities.

Capacity (MW)		Land cost	Distance to transmission line	Distance to road
250	Land cost	1	2	6
	Distance to transmission line	0.5	1	3
	Distance to road	0.167	0.333	1
	Land cost	1	4	8
500	Distance to transmission line	0.25	1	3
	Distance to road	0.125	0.333	1
	Land cost	1	8	9
1000	Distance to transmission line	0.125	1	3
	Distance to road	0.111	0.333	1

Table 3
Weights of site-based constraints.

	Solar radiation rate	**Land use**	**Slope**
Site-based weights	0.58	0.23	0.19

Table 4
Weights of cost-based constraints.

Cost-based	Land cost	Distance to transmission line	Distance to road
Weights for 250 MW	0.60	0.30	0.10
Weights for 500 MW	0.71	0.21	0.08
Weights for 1000 MW	0.79	0.15	0.06

3.1. Suitability maps for PV farms having different capacities

In order to evaluate the differences in suitability between large-scale PV farms with varying capacities, the suitability of farms with 250 MW, 500 MW, and 1000 MW capacities were assessed, as shown in Fig. 5(a)–(c). As can be seen, there are slight differences between the resulting suitability maps for different capacities. However, it is important to note that these raw maps do not fully capture the real-world situation, as they do not account for the capacity of the PV farm. As can be observed in the raw suitability maps, there are regions that appear suitable for PV farm development but are surrounded by restricted areas. These closed regions may not be suitable for development considering the required capacity of the PV farm and should be excluded even if they appear suitable on the raw map.

Capacity-based suitability maps for farms with capacities of 250 MW, 500 MW, and 1000 MW are presented in Fig. 5(d), (e), and (f), respectively. The comparative figure illustrates that the real suitable sites (Fig. 5(d)–(f)) are significantly smaller than the raw suitability maps (Fig. 5(a)–(c)). Moreover, the number of suitable locations decreases considerably with increasing capacity.

The results indicate that there are large, capacitive regions in the north and west of the Izmir province that are suitable for PV farm development. These regions have the potential to accommodate more than one PV farm with a capacity of 1000 MW. However, it is worth noting that the region to the west has low suitability, while the region to the north has partly over 80% suitability.

Table 6 presents comprehensive information on the suitability of various areas for the construction of solar PV panels, categorized by suitability rank and capacity-based standards as depicted in Fig. 5. The suitability ranks are expressed as percentages, and the table includes the corresponding areas in square kilometers for different capacity levels

Table 5
Summary of weights of constraints and indicators of their sub-criteria.

Site-based constraints (50%)				Cost-based constraints (50%)			
Criteria	Weight	Sub-criteria	Indicators	Criteria	Weight	Sub-criteria	Indicators
Solar radiation rate (kWh/m^2/day)	58	<4	4	Land cost ($/m^2)	60 (250 MW)71 (500 MW)79 (1000 MW)	<50	9
		4–4.2	5			50–100	8
		4.2–4.4	6			100–150	7
		4.4–4.6	7			150–200	6
		4.6–4.8	8			200–250	5
		>4.8	9			250–300	4
						300–350	3
						350–400	2
						>400	1
Land Use	23	Water	restrained	Distance totransmission line (km)	30 (250 MW)21 (500 MW)15 (1000 MW)	0–1	9
		Trees	restrained			1–2	8
		Flooded veg.	restrained			2–4	7
		Crops	restrained			4–8	6
		Built area	restrained			8–16	4
		Bare ground	8			>16	2
		Snow/ice	restrained				
		Rangeland	9				
Slope (%)	19	0–3	9	Distance toroad (km)	10 (250 MW)8 (500 MW)6 (1000 MW)	0–0.025	restrained
		3–6	8			0–1	9
		6–9	7			1–2	8
		9–12	4			2–4	7
		12–24	2			4–8	6
		>24	restrained			8–16	4
						>16	2

(250 MW, 500 MW, and 1000 MW). Notably, when the standard AHP is applied, approximately 77.5% of the regions are classified as unsuitable across all capacity levels. However, the percentage of unsuitable regions significantly increases when the capacities of the solar PV panels are considered. This is primarily due to the minimum land requirements associated with different capacity levels. In cases where a suitable area enclosed within restricted regions falls short of the necessary space for constructing a large-scale PV plant, that particular region is deemed unsuitable in the calculations that account for capacity. Similarly, the proportion of suitable regions decreases significantly when capacity is taken into consideration.

The high proportion of unsuitable areas can be attributed to the inclusion of restricted regions in the criteria list. Further examination of the sub-criteria reveals that these restricted zones primarily arise from considerations related to land cover and slope. While there are a few possible actions to reduce the number of unsuitable regions, such as constructing solar PV farms on lands designated for agricultural use or areas with slopes exceeding 24%, it is important to note that the government prohibits the installation of solar PV panels on agricultural lands. Additionally, constructing solar PV panels in regions with slopes higher than 24% may not be economically viable for the project.

3.2. *Optimality maps for PV farms having different capacities*

The suitability map and capacity-based suitability map are useful in identifying suitable sites for large-scale PV farms. The main disadvantage of these maps is that while the suitability map cannot account for the fact that a large-scale PV farm covers a large surface on the terrain, the capacity-based suitability map does not consider the real capacity of the PV farm. To find the suitable sites, a spatial analysis is carried out based on the pre-defined dimension of pixels which should be small for a detailed analysis. However, a large-scale PV farm covers a large surface on the terrain. After conducting a detailed spatial analysis, a set of adjacent pixels should be selected to form the large-scale PV farm. Disconnection between pixels or groups of pixels forming the PV farm is unacceptable due to possible serviceability and economic considerations. Besides, it is preferred to have a region of pixels close to each other to decrease maintenance costs and increase safety in emergency cases.

To address this challenge, the OBSG method was developed to determine the optimality rank of a point (pixel) on the suitability map. The OBSG method selects the optimal pixel among the possible adjacent pixels while growing the site to achieve a predefined PV capacity. The optimality condition is related to both the suitability of the pixel and the distance from the geometric center of the most recent site. This method is applied for every suitable pixel on the suitability map of PV farms, and the resulting map is called the optimality map.

The optimality map is different from the suitability map as it shows the optimality rank of a pixel on which a large-scale PV farm is constructed with a set of adjacent pixels, while suitability map shows the own suitability of every pixel on the map. Therefore, the optimality of a pixel is based on the suitability of adjacent pixels. The optimality map is more comprehensive than the suitability map for the site selection of large-scale PV farms. Fig. 6(a), (b), and (c) depict the optimality maps of large-scale PV farms with 250 MW, 500 MW, and 1000 MW capacities, respectively.

3.3. *Sequentially allocated optimal large-scale PV farms having different capacities*

In addition to the optimality map achieved by the OBSG method, an alternative way of demonstrating the optimality of site selection for large-scale PV farms is through sequential allocation. This involves selecting the best pixel as the seeding location for each successive allocation of a large-scale PV farm. The best pixel is determined by applying the OBSG method to every suitable pixel on the suitability map, resulting in the optimality rank of each pixel. The best-ranked pixel is then chosen as the location for the next large-scale PV farm. This process is repeated until the desired number of large-scale PV farms with the same capacity is reached. In each successive allocation, the best new location on the suitability map consisting existing large-scale PV farms is found. The resultant suitable locations are given in Fig. 7.

The disadvantage of sequential allocation is that it assumes that the optimality of pixels covered by a large-scale PV farm is the same (refer to Fig. 7), unlike the suitability values obtained from the optimality map (refer to Fig. 6). Besides, there are some regions remaining from the successive large-scale PV farm allocations and these regions seem to be unsuitable. Nonetheless, the sequential allocation method has the

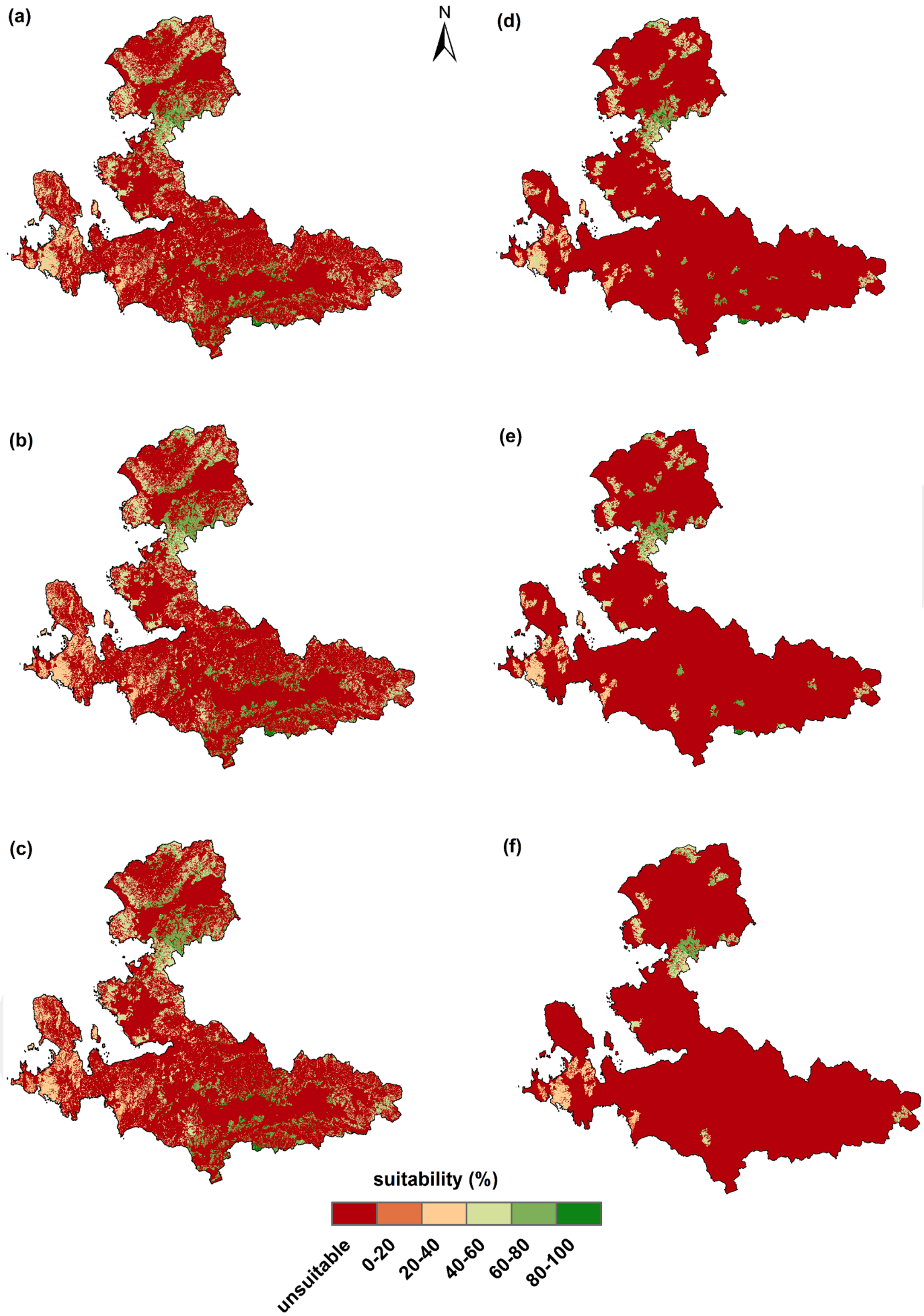

Fig. 5. Suitability maps of (a) 250 MW, (b) 500 MW and (c) 1000 MW PV farm capacities and capacity-based suitability maps of (d) 250 MW, (e) 500 MW and (f) 1000 MW PV farm capacities.

advantage of selecting the best site for each successive allocation of a large-scale PV farm, since the previously selected area is disregarded in the next PV selection.

The number of sequentially allocated PV farms for 250 MW, 500 MW, and 1000 MW capacities are 210, 80, and 30, respectively. Assuming a farm with a 1 MW capacity covers an area of 15000 m^2, the total areas covered by these sequentially located PV farms are 785.5 km^2, 600 km^2 and 450 km^2 for respective capacities.

4. Conclusions and future works

The AHP method was integrated with GIS to identify suitable locations for large-scale PV farms in a case study situated in İzmir, Türkiye. In addition to the widely used constraints in the AHP, the land cost was

Table 6
Standard and capacity-based suitability results.

Suitability Rank (%)	Standard (km^2)			Capacity-based (km^2)		
	250 MW	500 MW	1000 MW	250 MW	500 MW	1000 MW
Unsuitable	9213 (77.48%)	9213 (77.48%)	9213 (77.48%)	10,782 (90.68%)	11,011 (92.60%)	11,276 (94.83%)
0–20	9 (0.07%)	25 (0.21%)	73 (0.61%)	3 (0.02%)	4 (0.03%)	33 (0.27%)
20–40	529 (4.45%)	574 (4.82%)	567 (4.77%)	243 (2.04%)	261 (2.20%)	186 (1.57%)
40–60	1397 (11.75%)	1246 (10.48%)	1152 (9.69%)	580 (4.88%)	378 (3.18%)	244 (2.05%)
60–80	707 (5.95%)	788 (6.63%)	837 (7.04%)	263 (2.21%)	218 (1.83%)	144 (1.21%)
80–100	36 (0.31%)	46 (0.38%)	50 (0.42%)	20 (0.17%)	16 (0.14%)	5 (0.04%)

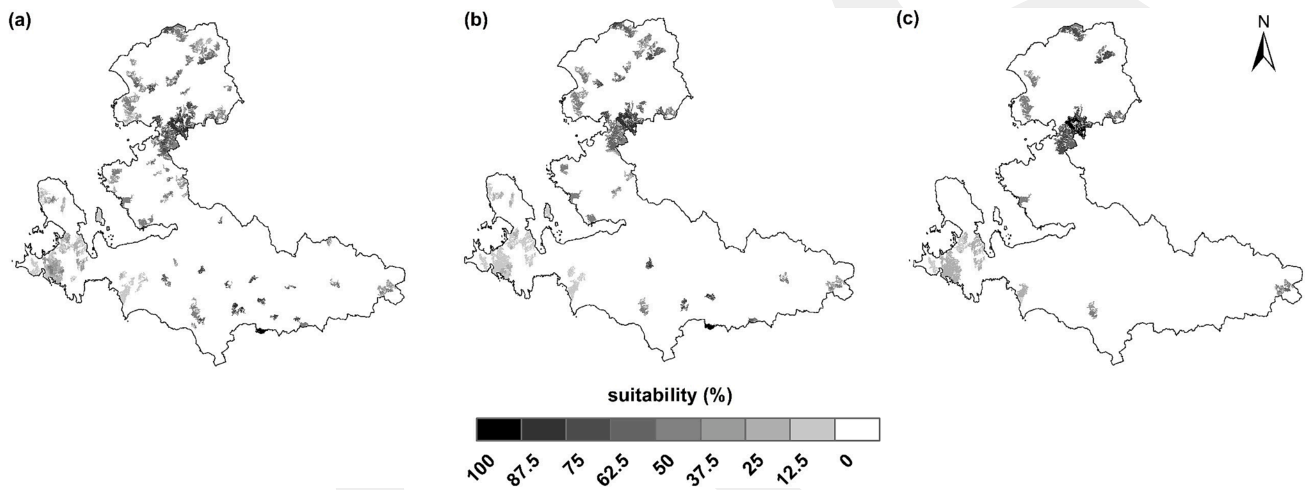

Fig. 6. Optimality maps of (a) 250 MW, (b) 500 MW and (c) 1000 MW PV farm capacities.

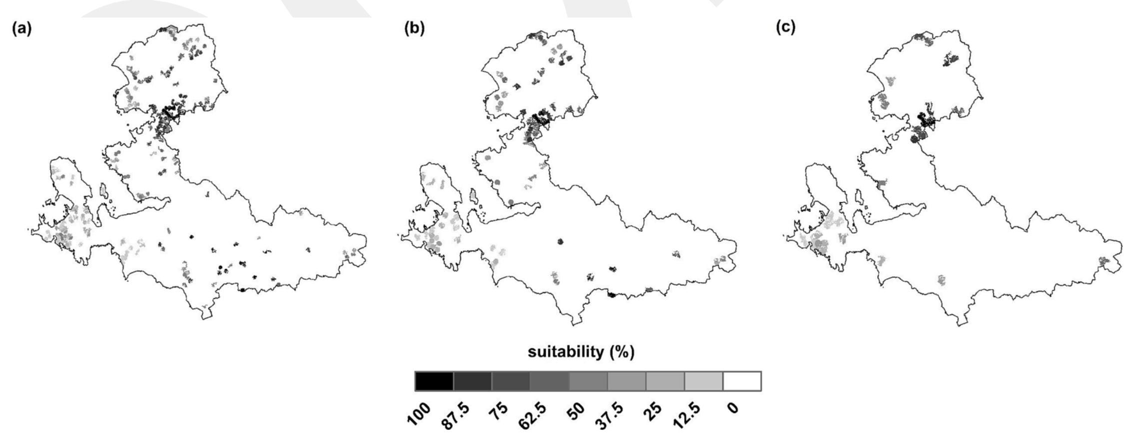

Fig. 7. Optimality ranks of sequentially allocated PV farms having (a) 250 MW, (b) 500 MW and (c) 1000 MW capacities.

included since it becomes more important in the selection of large-scale PV sites. Besides two novel methods were proposed for selecting optimal sites for large-scale PV farm allocations: the OBSG method and sequential allocation. The results of the proposed methods were compared with the suitability map obtained from the simple GIS works. In addition, the suitability maps were modified to obtain capacity-based suitability maps. The capacity-based suitability maps provide a more realistic representation of suitable locations for large-scale PV farms, taking into account the capacity of the farm. The OBSG method and resultant optimality maps offer a more comprehensive approach to site selection by considering both the suitability of adjacent pixels and the distance from the geometric center of the most recent site. Sequential allocation offers an alternative approach to selecting optimal sites, but it assumes that the optimality of pixels covered by a large-scale PV farm is the same. Overall, the proposed methods provide valuable insights for selecting suitable and optimal sites for large-scale PV farms.

As a limitation of the proposed method, it should be noted that during the sequential allocation of solar farms with the same capacity, some regions may be absent from the allocation process due to not meeting the minimum area requirements of the same capacity. It is crucial to understand that the purpose of this sequential allocation is to rank sites exclusively for farms with the same capacity. Therefore, the absence of certain regions in the allocation does not imply their unsuitability for solar farm development. It simply indicates that these missing regions are not suitable for solar PV farms with the same capacity being considered in the allocation process. In addition, the present study focused on investigating solar PV farms with capacities of 250, 500, and 1000 MW. It is crucial to conduct an investigation based on the specific capacity requirements of each individual project.

Future research could focus on further investigating restriction zones, particularly slopes, and exploring the suitable areas when solar PV farms are constructed on lands with higher slopes as technology advances. Furthermore, it may be helpful to utilize various Computational Fluid Dynamics (CFD) software ([49]), to determine regions that may be susceptible to natural hazards like floods, dam-breaks, or landslides. Then, these regions can be excluded from consideration when determining suitable sites for solar PV farms. Additionally, an intriguing aspect to consider would be incorporating carbon dioxide emissions resulting from the transportation of solar PV farms into the decision criteria list.

Declaration of Competing Interest

The authors declare that they have no known competing financial interests or personal relationships that could have appeared to influence the work reported in this paper.

References

[1] Abdul-Wahab, S., Charabi, Y., Al-Mahruqi, A.M., Osman, I., Osman, S., 2019. Selection of the best solar photovoltaic (PV) for Oman. Sol. Energy 188, 1156–1168. https://doi.org/10.1016/j.solener.2019.07.018.

[2] Adiguzel, F., Bozdogan Sert, E., Dinc, Y., Cetin, M., Gungor, S., Yuka, P., Sertkaya Dogan, O., Kaya, E., Karakaya, K., Vural, E., 2022. Determining the relationships between climatic elements and thermal comfort and tourism activities using the tourism climate index for urban planning: a case study of Izmir Province: Tourism climate index for urban planning. Theor. Appl. Climatol. 147, 1105–1120. https://doi.org/10.1007/s00704-021-03874-9.

[3] Al Garni, H.Z., Awasthi, A., 2018. Solar PV Power Plants Site Selection: A Review, in: Advances in Renewable Energies and Power Technologies. Elsevier, pp. 57–75. doi: 10.1016/B978-0-12-812959-3.00002-2.

[4] Al Garni, H.Z., Awasthi, A., 2017. A Fuzzy AHP and GIS-based approach to prioritize utility-scale solar PV sites in Saudi Arabia. In: 2017 IEEE International Conference on Systems, Man, and Cybernetics, SMC 2017. Institute of Electrical and Electronics Engineers Inc., pp. 1244–1249. https://doi.org/10.1109/SMC.2017.8122783

[5] Alami Merrouni, A., Elwali Elalaoui, F., Mezrhab, A., Mezrhab, A., Ghennioui, A., 2018. Large scale PV sites selection by combining GIS and Analytical Hierarchy Process. Case study: Eastern Morocco. Renew. Energy 119, 863–873. https://doi.org/10.1016/j.renene.2017.10.044.

[6] Al-Ghussain, L., Taylan, O., Abujubbeh, M., Hassan, M.A., 2023. Optimizing the orientation of solar photovoltaic systems considering the effects of irradiation and cell temperature models with dust accumulation. Sol. Energy 249, 67–80. https://doi.org/10.1016/j.solener.2022.11.029.

[7] Aly, A., Jensen, S.S., Pedersen, A.B., 2017. Solar power potential of Tanzania: Identifying CSP and PV hot spots through a GIS multicriteria decision making analysis. Renew. Energy 113, 159–175. https://doi.org/10.1016/j.renene.2017.05.077.

[8] Anser, K.M., Mohsin, M., Abbas, Q., Imran, &, Chaudhry, S., 2020. Assessing the integration of solar power projects: SWOT-based AHP-F-TOPSIS case study of Turkey. Environ. Sci. Pollut. Res. 27, 31737–31749. doi: 10.1007/s11356-020-09092-6/Published.

[9] Badi, I., Pamucar, D., Gigović, L., Tatomirović, S., 2021. Optimal site selection for sitting a solar park using a novel GIS- SWA'TEL model: A case study in Libya. Int. J. Green Energy 18, 336–350. https://doi.org/10.1080/15435075.2020.1854264.

[10] Colak, H.E., Memisoglu, T., Gercek, Y., 2020. Optimal site selection for solar photovoltaic (PV) power plants using GIS and AHP: A case study of Malatya Province, Turkey. Renew. Energy 149, 565–576. https://doi.org/10.1016/j.renene.2019.12.078.

[11] Copernicus Land Monitoring Service, 2023. CLC 2018 [WWW Document]. URL https://land.copernicus.eu/pan-european/corine-land-cover/clc2018 (accessed 5.9.23).

[12] Cousse, J., 2021. Still in love with solar energy? Installation size, affect, and the social acceptance of renewable energy technologies. Renew. Sustain. Energy Rev. 145, 111107.

[13] Cranmer, A., Ericson, J.D., Ebers Broughel, A., Bernard, B., Robicheaux, E., Podolski, M., 2020. Worth a thousand words: Presenting wind turbines in virtual reality reveals new opportunities for social acceptance and visualization research. Energy Res. Soc. Sci. 67, 101507.

[14] Debaleena, M., Martin, P., 2019. Analysis of land availability for utility-scale power plants and assessment of solar photovoltaic development in the state of Arizona, USA. Renew. Energy 134, 1213–1231.

[15] Dhunny, A.Z., Doorga, J.R.S., Allam, Z., Lollchund, M.R., Boojhawon, R., 2019. Identification of optimal wind, solar and hybrid wind-solar farming sites using fuzzy logic modelling. Energy 188, 116056.

[16] EuroGeographics, 2023. General Directorate of Mapping - Turkey [WWW Document]. URL https://eurogeographics.org/member/general-command-of-mapping/ (accessed 5.9.23).

[17] European Commission, 2019. The European green deal [WWW Document]. URL https://commission.europa.eu/strategy-and-policy/priorities-2019-2024/european-green-deal/delivering-european-green-deal_en (accessed 1.2.23).

[18] Ferreira, A., Kunh, S.S., Fagnani, K.C., De Souza, T.A., Tonezer, C., Dos Santos, G.R., Coimbra-Araújo, C.H., 2018. Economic overview of the use and production of photovoltaic solar energy in Brazil. Renew. Sustain. Energy Rev. 81, 181–191.

[19] Günen, M.A., 2021. A comprehensive framework based on GIS-AHP for the installation of solar PV farms in Kahramanmaraş, Turkey. Renew. Energy 178, 212–225. https://doi.org/10.1016/j.renene.2021.06.078.

[20] International Energy Agency, 2021. Turkey 2021 - energy policy review.

[21] İzmir Development Agency, 2013. İzmir Regional Plan 2014-2023. İzmir.

[22] Kannan, N., Vakeesan, D., 2016. Solar energy for future world: - A review. Renew. Sustain. Energy Rev. 62, 1092–1105.

[23] Lopez, A., Roberts, B., Heimiller, D., Blair, N., Porro, G., 2012. U.S. Renewable Energy Technical Potentials: A GIS-Based Analysis. Colorado.

[24] Merrouni, A.A., Elalaoui, E.F., Ghennioui, A., Mezrhab, A., Mezrhab, A., 2018. A GIS-AHP combination for the sites assessment of large-scale CSP plants with dry and wet cooling systems. Case study: Eastern Morocco. Solar Energy 166, 2–12. https://doi.org/10.1016/j.solener.2018.03.038.

[25] Merrouni, A.A., Elalaoui, E.F., Mezrhab, A., Mezrhab, A., Ghennioui, A., 2018. Large scale PV sites selection by combining GIS and Analytical Hierarchy Process. Case study: Eastern Morocco. Renew Energy 119, 863–873. https://doi.org/10.1016/j.renene.2017.10.044.

[26] Mondino, B.E., Fabrizio, E., Chiabrando, R., 2015. Site selection of large ground-mounted photovoltaic plants: A GIS decision support system and an application to Italy. Int. J. Green Energy 12, 515–525. https://doi.org/10.1080/15435075.2013.858047.

[27] Mukhtarov, S., Yüksel, S., Dinçer, H., 2022. The impact of financial development on renewable energy consumption: Evidence from Turkey. Renew. Energy 187, 169–176. https://doi.org/10.1016/j.renene.2022.01.061.

[28] Noorollahi, Y., Ghenaatpisheh Senani, A., Fadaei, A., Simaee, M., Moltames, R., 2022. A framework for GIS-based site selection and technical potential evaluation of PV solar farm using Fuzzy-Boolean logic and AHP multi-criteria decision-making approach. Renew. Energy 186, 89–104. https://doi.org/10.1016/j.renene.2021.12.124.

[29] Noorollahi, Y., Yousefi, H., Mohammadi, M., 2016. Multi-criteria decision support system for wind farm site selection using GIS. Sustainable Energy Technol. Assess. 13, 38–50. https://doi.org/10.1016/j.seta.2015.11.007.

[30] Open Street Map, 2023. OpenStreetMap [WWW Document]. URL https://www.openstreetmap.org/copyright/en (accessed 5.9.23).

[31] Pamučar, D., Stević, Ž., Sremac, S., 2018. A new model for determining weight coefficients of criteria in MCDM models: Full Consistency Method (FUCOM). Symmetry (Basel) 10 (9), 393.

[32] Rediske, G., Siluk, J.C.M., Gastaldo, N.G., Rigo, P.D., Rosa, C.B., 2019. Determinant factors in site selection for photovoltaic projects: A systematic review. Int. J. Energy Res. 43 (5), 1689–1701.

[33] Rediske, G., Siluk, J.C.M., Michels, L., Rigo, P.D., Rosa, C.B., Cugler, G., 2020. Multi-criteria decision-making model for assessment of large photovoltaic farms in Brazil. Energy 197, 117167.

[34] Saaty, T.L., 2008. Decision making with the analytic hierarchy process. Int. J. Services Sci. 1, 83–98.

[35] Saaty, T.L., 1980. The analytic hierarchy process: planning, priority setting, resource allocation. McGraw-Hill International Book Co.

[36] Sánchez-Lozano, J.M., Henggeler Antunes, C., García-Cascales, M.S., Dias, L.C., 2014. GIS-based photovoltaic solar farms site selection using ELECTRE-TRI: Evaluating the case for Torre Pacheco, Murcia, Southeast of Spain. Renew. Energy 66, 478–494. https://doi.org/10.1016/j.renene.2013.12.038.

[37] Saracoglu, B.O., 2020. Location selection factors of concentrated solar power plant investments. Sustain. Energy Grids Networks 22, 100319.

[38] Saraswat, S.K., Digalwar, A.K., Yadav, S.S., Kumar, G., 2021. MCDM and GIS based modelling technique for assessment of solar and wind farm locations in India. Renew. Energy 169, 865–884. https://doi.org/10.1016/j.renene.2021.01.056.

[39] Song, B., Kang, S., 2016. A Method of assigning weights using a ranking and nonhierarchy comparison. Adv. Decis. Sci. 2016, 1–9.

[40] Sözen, A., Arcaklioğlu, E., Özalp, M., Kanit, E.G., 2004. Use of artificial neural networks for mapping of solar potential in Turkey. Appl. Energy 77, 273–286. https://doi.org/10.1016/S0306-2619(03)00137-5.

[41] Spyridonidou, S., Sismani, G., Loukogeorgaki, E., Vagiona, D.G., Ulanovsky, H., Madar, D., 2021. Sustainable spatial energy planning of large-scale wind and pv

farms in israel: A collaborative and participatory planning approach. Energies (Basel) 14 (3), 551.
[42] Sütterlin, B., Siegrist, M., 2017. Public acceptance of renewable energy technologies from an abstract versus concrete perspective and the positive imagery of solar power. Energy Policy 106, 356–366. https://doi.org/10.1016/j.enpol.2017.03.061.
[43] Suuronen, A., Lensu, A., Kuitunen, M., Andrade-Alvear, R., Celis, N.G., Miranda, M., Perez, M., Kukkonen, J.V.K., 2017. Optimization of photovoltaic solar power plant locations in northern Chile. Environ. Earth Sci. 76 https://doi.org/10.1007/s12665-017-7170-z.
[44] Tahri, M., Hakdaoui, M., Maanan, M., 2015. The evaluation of solar farm locations applying Geographic Information System and Multi-Criteria Decision-Making methods: Case study in southern Morocco. Renew. Sustain. Energy Rev. 51, 1354–1362.
[45] T.C. Enerji ve Tabii Kaynaklar Bakanlığı, 2022. Güneş [WWW Document]. URL https://enerji.gov.tr/bilgi-merkezi-enerji-gunes (accessed 5.9.23).
[46] Uyan, M., 2017. Optimal site selection for solar power plants using multi-criteria evaluation: a case study from the Ayranci region in Karaman, Turkey. Clean Techn. Environ. Policy 19 (9), 2231–2244.
[47] World Nuclear Association, 2022. Carbon dioxide emissions from electricity [WWW Document]. World Nuclear Association. URL https://www.world-nuclear.org/information-library/energy-and-the-environment/carbon-dioxide-emissions-from-electricity.aspx (accessed 1.2.23).
[48] Zoghi, M., Houshang Ehsani, A., Sadat, M., javad Amiri, M., Karimi, S., 2017. Optimization solar site selection by fuzzy logic model and weighted linear combination method in arid and semi-arid region: A case study Isfahan-IRAN. Renew. Sustain. Energy Rev. 68, 986–996.
[49] D. Velioglu, N. Tokyay, A.E. Dincer, 2015. A numerical and experimental study on the characteristics of hydraulic jumps on rough beds, in: E-proceedings of the 36th IAHR World Congress, Hague, Netherlands, pp. 1–9.